

# Preparation of $(\text{Tb}_{0.8}\text{Y}_{0.2})_3\text{Al}_5\text{O}_{12}$ transparent ceramic as novel magneto-optical isolator material

Chong Chen (陈冲)<sup>1</sup>, Yi Ni (倪屹)<sup>2</sup>, Shengming Zhou (周圣明)<sup>1\*</sup>,  
Hui Lin (林辉)<sup>1</sup>, and Xuezhuan Yi (易学专)<sup>1</sup>

<sup>1</sup>Key Laboratory of Materials for High Power Laser, Shanghai Institute of Optics and Fine Mechanics,  
Chinese Academy of Sciences, Shanghai 201800, China

<sup>2</sup>School of Internet of Things Engineering, Jiangnan University, Wuxi 214122, China

\*Corresponding author: zhousm@siom.ac.cn

Received June 18, 2012; accepted September 4, 2012; posted online January 21, 2013

The ion substitution characteristics of  $\text{Y}^{3+}$ -doped  $(\text{Tb}_{0.8}\text{Y}_{0.2})_3\text{Al}_5\text{O}_{12}$  transparent ceramics synthesized by a solid-state reaction and vacuum sintering are investigated. The sample sintered at 1680 °C exhibits the best optical properties, yielding a transmittance >75% from 900 to 1600 nm. The Verdet constant of this sample at 632.8 nm is  $-108.79 \text{ rad}\cdot\text{T}^{-1}\cdot\text{m}^{-1}$ . X-ray diffraction (XRD) results show that all of the samples have a pure garnet crystal structure without secondary phases. The microstructure of the samples reveals homogeneous grain sizes that averages  $<10 \mu\text{m}$ .

OCIS codes: 160.3820, 160.4670.

doi: 10.3788/COL201311.021601.

Magneto-optical materials are important components of Faraday isolators in high-power lasers. Today, the most commonly used Faraday magneto-optical material in the visible (VIS) and near-infrared (NIR) regions is the terbium gallium garnet ( $\text{Tb}_3\text{Ga}_5\text{O}_{12}$ , TGG) single crystal<sup>[1,2]</sup>. In fact, the terbium aluminum garnet ( $\text{Tb}_3\text{Al}_5\text{O}_{12}$ , TAG) single crystal is much better choice for its large Verdet constant.<sup>[3,4]</sup> However, the growth of TAG single crystals from the melt is extremely difficult because of the incongruent melting nature of TAG and its unstable phase<sup>[5]</sup>. Considerable efforts have been devoted to the improvement of the quality of TAG-based single crystals. For example, some researchers have used  $\text{Lu}^{3+}$ ,  $\text{Sc}^{3+}$ , and  $\text{Yb}^{3+}$  ions to partially substitute  $\text{Tb}^{3+}$  or  $\text{Al}^{3+}$  ions<sup>[6,7]</sup> and stabilize the garnet phase. Other scholars have developed new synthesis methods, such as the hybrid floating zone method<sup>[8]</sup>. However, the utilization of TAG single crystals remains limited by the size and optical quality of the crystals obtained. Thus, TAG single crystals are unavailable in the commercial market.

In theory, TAG ceramics should be able to avoid incongruent melting problems because their fabrication temperature is well below their melting point. Over the past two decades, several studies have shown that the transparent ceramic may replace its single crystal counterpart because of its excellent properties<sup>[9,10]</sup>. The TGG ceramic was first reported in 2003<sup>[11]</sup>, and recent studies had shown that TGG transparent ceramics exhibited qualities similar to those of single crystals<sup>[12,13]</sup>. The synthesis of TAG transparent ceramics has also been studied<sup>[14]</sup>. The Verdet constant of TAG transparent ceramics fabricated in Ref. [14] is  $-172.72 \text{ rad}\cdot\text{T}^{-1}\cdot\text{m}^{-1}$  at 632.8 nm, which is approximately equal to that of a TAG single crystal, and 75% transmittance can be achieved within the 400–1600 nm region. These findings indicate that the TAG transparent ceramic may be a potential magneto-optical material.

The yttrium iron garnet (YIG) single crystal is the

most commonly used Faraday isolator material in the 1.1–5.5  $\mu\text{m}$  region; however, it cannot be used in the VIS and NIR regions because of its strong absorption<sup>[15]</sup>. In 1973, the Faraday rotation angle in the VIS and NIR regions of  $\text{Bi}^{3+}$ -doped YIG was found to be one to two orders of magnitude larger than that of pure YIG<sup>[16–18]</sup>. In 1988,  $\text{Ce}^{3+}$ -doped YIG was investigated and its magneto-optical properties were found to be more efficient than those of Bi:YIG<sup>[19]</sup>. Previous works have also investigated  $\text{Tb}^{3+}$ -doped  $\text{Y}_3\text{Al}_5\text{O}_{12}$  (YAG)<sup>[20,21]</sup>. In this letter, we use  $\text{Y}^{3+}$  to partially replace  $\text{Tb}^{3+}$  and investigate the performance of  $(\text{Tb}_{0.8}\text{Y}_{0.2})_3\text{Al}_5\text{O}_{12}$  (Y-TAG) transparent ceramics.

High-purity  $\text{Al}_2\text{O}_3$  (99.999%),  $\text{Y}_2\text{O}_3$  (99.999%), and  $\text{Tb}_4\text{O}_7$  (99.999) commercial powders were weighed according to the designed  $(\text{Tb}_{0.8}\text{Y}_{0.2})_3\text{Al}_5\text{O}_{12}$  composition. Ethyl orthosilicate (0.4 wt%) and magnesia (0.008 wt%) were also added to the powder mixture. The powders were mixed by ball milling in ethanol for 24 h. Afterwards, the mixture was dried at 80 °C for 48 h, uniaxially pressed into plates at 10 MPa, and then subjected to cold isostatic pressing at 200 MPa. The green bodies were pre-sintered in air at 600 °C for 3 h to remove organic ingredients. The plates were sintered at 1650, 1665, 1680, 1695, and 1710 °C under a base pressure of approximately  $1.0\times 10^{-3}$  Pa for 11 h. The obtained transparent ceramic samples were labeled S1, S2, S3, S4, and S5. All specimens were polished on both sides to the same thickness. The optical transmittance spectra of the samples were measured on an ultraviolet/VIS/NIR spectrophotometer (V-570-JASCO, Japan) and their crystal structure was investigated by X-ray diffraction (XRD) on an Ultima IV instrument (Rigaku, Japan). The microstructures were analyzed by scanning electron microscopy (SEM) on an Auriga-39-40 system (Auriga, Germany). The Verdet constant at 632.8 nm was measured using a home-made instrument that included a He-Ne laser, two polarizers, and an electromag-

net. All of the characterization methods were conducted at room temperature.

A photograph of Y-TAG transparent ceramic samples is shown in Fig. 1. With the exception of S5, which is translucent, the letters under all of the samples can be seen clearly, particularly in S2 and S3. Figure 2 shows the XRD  $\theta$ - $2\theta$  scanning patterns of the samples. All of the samples show a pure phase that is almost identical to the standard cubic TAG phase. The diffraction peaks slightly shifted at different sintering temperatures. S1 showed the largest shift and the tendency approached to the phase of pure yttrium aluminum garnet (YAG). Figure 2 also illustrates that the  $Y^{3+}$  ion can be heavily doped into the TAG lattice.

The optical transmittance spectra of the transparent ceramics are shown in Fig. 3. The transmittance of the samples initially increased and reached a maximum of  $>75\%$  at 900–1600 nm in S3 and then decreased in S4

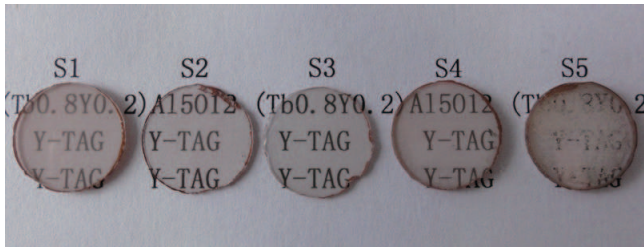


Fig. 1. Picture of the double-side polished Y-TAG transparent ceramic samples sintered at different temperatures.

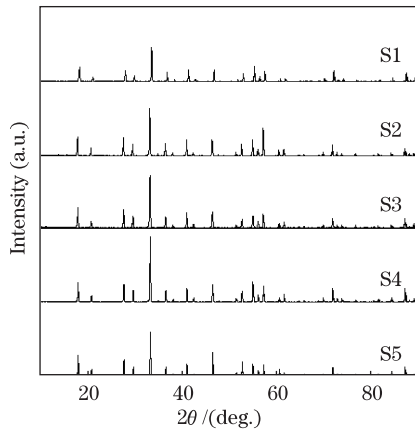


Fig. 2. XRD patterns for all the transparent ceramic samples.

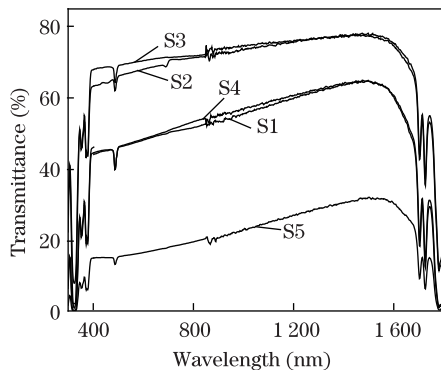


Fig. 3. Optical transmittance of the polished transparent ceramic samples.

and S5. Variations in the optical transmittance of all of the samples were consistent with the appearance of the samples shown in Fig. 1. At approximately 900–1600 nm, the transmittances of S2 and S3 reached 77%, indicating that doping with  $Y^{3+}$  ions improves the optical properties of TAG. The optical transmittance spectra also indicate that Y-TAG transparent ceramics are sensitive to relatively high sintering temperatures. The transmittance of S5 was  $<30\%$  in the VIS and NIR regions while the sintering temperature was  $15^\circ\text{C}$  higher than S4. Although its intensity was relatively weak, an absorption peak at approximately 484 nm, which was attributed to the  $Tb^{3+}:^7F_6 \rightarrow ^5D_4$  transition<sup>[14]</sup>, was also detected. Peaks at approximately 880 nm were brought about by the change in excitation source during measurement. In this letter, the only varying factor was the sintering temperature; thus, the optical properties of the transparent ceramics could be further enhanced if we optimize the synthesis process. For example, we could improve the granularity of the raw material powders and adjust the sintering schedule, among others.

The microstructure of the ceramic samples was measured by SEM after thermal etched at  $1400^\circ\text{C}$  for 10 h (Fig. 4). The grain size of all of the samples was comparatively homogeneous and without abnormal grain growth. The average grain size was relatively small but the pores were still observable. The average grain sizes were 8.72 and  $9.44\ \mu\text{m}$  for S1 and S4, respectively, and few pores were observed (Figs. 4(a) and (d)). The pores in S2 and S3 were greatly reduced, consistent with their improved optical properties. The average grain sizes of S3 and S2 were 5.46 and  $8.93\ \mu\text{m}$ , respectively. Small grains attached to the surface of S3 may have been caused by thermal etching. The microstructure of S5 illustrated in Fig. 4(e) indicates the poor optical properties of the sample. While many pores were enclosed in the grains and various small grains were embedded in the grain boundaries, which were marked by squares, the average

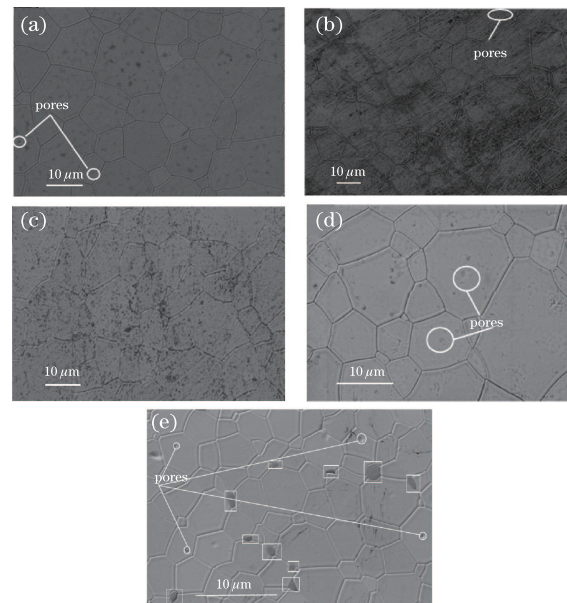


Fig. 4. SEM photographs for the thermal-etched polished surface of the samples (a) S1, (b) S2, (c) S3, (d) S4, and (e) S5.

grain size was only  $3.46\ \mu\text{m}$ , the smallest among all of the samples. The SEM image revealed a smaller average grain size for  $\text{Y}^{3+}$  ion-doped TAG transparent ceramics, which indicated that it could optimize the microstructure of TAG. The SEM results further indicate that the sintering temperature does not exhibit an evident relationship with the grain size.

The Verdet constant of S2 at  $632.8\ \text{nm}$  measured at room temperature was  $-108.79\ \text{rad}\cdot\text{T}^{-1}\cdot\text{m}^{-1}$ , which was approximately 37% lower than that of a reported TAG transparent ceramic sample<sup>[14]</sup> and 19% lower than that of TGG transparent ceramic<sup>[13]</sup>. Thus, doping TAG transparent ceramics with  $\text{Y}^{3+}$  ions significantly affects the magneto-optical properties of the resulting material.

In conclusion,  $\text{Y}^{3+}$ -doped TAG transparent ceramic samples are achieved by a solid-state reaction and vacuum sintering. A stable TAG phase is obtained over a broad sintering temperature range (from  $1650$  to  $1710\ ^\circ\text{C}$ ). The optical quality of TAG transparent ceramics can be improved by doping with  $\text{Y}^{3+}$ . The transmittances of S2 and S3 reach 77% in the NIR region. The average grain size of the samples is  $<10\ \mu\text{m}$ . Doping with  $\text{Y}^{3+}$  decreases the magneto-optical properties of TAG and its Verdet constant is reduced to  $-108.79\ \text{rad}\cdot\text{T}^{-1}\cdot\text{m}^{-1}$  at  $632.8\ \text{nm}$ . Future studies can focus on determining other ions that can improve the quality of TAG transparent ceramics.

This work was supported by the National Natural Science Foundation of China (Nos. 51172254 and 51202269) and the Science and Technology Commission of Shanghai Municipality (No. 10JC1415700).

## References

1. A. V. Voitovich, E. V. Katin, L. Mukhin, O. V. Palashov, and E. A. Khazanov, *Quantum Electron.* **37**, 471 (2007).
2. A. A. Kaminskii, H. J. Eichler, P. Reiche, and R. Uecker, *Laser Phys. Lett.* **2**, 489 (2005).
3. C. B. Rubinstein, L. G. Van Uitert, and W. H. Grodkiewicz, *J. Appl. Phys.* **35**, 3069 (1964).
4. F. J. Sansalone, *Appl. Opt.* **10**, 2329 (1971).
5. S. Ganschow, D. Klimm, P. Reiche, and R. Uecker, *Cryst. Res. Technol.* **34**, 615 (1999).
6. V. I. Chani, A. Yoshikawa, H. Machida, and T. Fukuda, *J. Cryst. Growth* **212**, 469 (2000).
7. K. Shimamura, T. Kito, E. Castel, A. Latynina, P. Molina, E. G. Villora, P. Mythili, P. Veber, J. P. Cham-inade, A. Funaki, T. Hatanaka, and K. Naoe, *Cryst. Growth Design* **10**, 3466 (2010).
8. M. Geho, T. Sekijima, and T. Fujii, *J. Cryst. Growth* **267**, 188 (2004).
9. A. Ikesue, I. Furusato, and K. Kamata, *J. Am. Ceram. Soc.* **78**, 225 (1995).
10. B. Jiang, T. Huang, Y. Wu, W. Liu, and Y. Pan, *Chin. Opt. Lett.* **7**, 505 (2009).
11. E. A. Khazanov, *Proc. SPIE* **4968**, 115 (2003).
12. R. Yasuhara, S. Tokita, J. Kawanaka, T. Kawashima, H. Kan, H. Yagi, H. Nozawa, T. Yanagitani, Y. Fujimoto, H. Yoshida, and M. Nakatsuka, *Opt. Express* **15**, 11255 (2007).
13. H. Yoshida, K. Tsubakimoto, Y. Fujimoto, K. Mikami, H. Fujita, N. Miyanaga, H. Nozawa, H. Yagi, T. Yanagitani, Y. Nagata, and H. Kinoshita, *Opt. Express* **19**, 15181 (2011).
14. H. Lin, S. M. Zhou, and H. Teng, *Opt. Mater.* **33**, 1833 (2011).
15. J. F. Dillon, *J. Appl. Phys.* **29**, 539 (1958).
16. H. Takeuchi, K. Shinaga and S. Taniguchi, *Jpn. J. Appl. Phys.* **44**, 4789 (1973).
17. D. E. Lacklison, G. B. Scott, H. I. Ralph, and J. L. Pace, *IEEE Trans. Magnet.* **9**, 457 (1973).
18. J. Bremer and V. Vaicikauskas, *J. Appl. Phys.* **89**, 6177 (2001).
19. M. Gomi and K. Satoh, *Jpn. J. Appl. Phys.* **27**, 1536 (1988).
20. D. Boal, P. Grunberg, and J. A. Koningstein, *Phys. Rev. B* **7**, 4757 (1973).
21. U. V. Valiev, J. B. Gruber, B. Zandi, U. R. Rustamov, A. S. Rakhmatov, D. R. Dzhuraev, and N. M. Narzullaev, *Physica Status Solidi B-Basic Solid State Physics* **242**, 933 (2005).